Autism Spectrum Disorder Prediction Using TSM-BFC and a Combined CNN–GRU Model Based on the EEG Image Dataset

Ambika Rani Subhash
Department of Information Science and Engineering, BMS Institute of Technology and Management, Bengaluru, India | School of Computer Science and Engineering, REVA University, Bengaluru, India
ambikasubash@bmsit.in (corresponding author)

U. M. Ashwinkumar
School of Computer Science and Engineering, REVA University, Bengaluru, India
ashwinkumar.um@reva.edu.in

Received: 16 June 2025 | Revised: 7 July 2025 and 11 July 2025 | Accepted: 13 July 2025

 DOI: https://doi.org/10.48084/etasr.12757

ABSTRACT

This work focuses on enhancing the detection of Autism Spectrum Disorder (ASD) by analyzing brain connectivity patterns, as the proper connectivity between the various brain regions is necessary for regular cognition. Neurological disease diagnostics has made extensive use of Electroencephalography (EEG). Frequency-related features have been the main focus of earlier research on the use of EEG data to diagnose ASD. Most previous studies divided the data into time slices or sliding windows. However, there is a chance that these data augmentation methods contaminate the testing with training data. This study presents a novel technique for identifying ASD using EEG data to get around this problem. Convolutional Neural Networks (CNNs) and Gated Recurrent Units (GRUs) were used to create and implement a model for diagnosing ASD, achieving a classification accuracy of 96.4%.

Keywords-Autism Spectrum Disorder (ASD); Electroencephalography (EEG); Convolutional Neural Network (CNN); Gated Recurrent Unit (GRU); deep learning

I. INTRODUCTION

Autism Spectrum Disorder (ASD) is a neurodevelopmental disorder that appears early in childhood, and its prevalence has gradually increased over time. According to the National Center for Health Statistics, about 1 in 36 children had ASD by 2016 [1]. People with ASD may experience long-term effects if they are not diagnosed and treated promptly. As a result, the need for dependable and effective diagnostic assistance systems is increasing. The ADOS, M-CHAT, and ADI-R are just a few of the behavioral tests and clinical observations that have historically been used to diagnose ASD [2]. However, these evaluations take a long time, and subjective responses can have an impact. To support diagnosis, researchers examine the underlying variations in brain activity between people with and without ASD since the development of neuroimaging technologies such as MRI, fMRI, and EEG [3].

Abnormal connections between brain regions are frequently associated with the cognitive difficulties associated with ASD. Normal brain function depends on these areas communicating well with each other. People with ASD often exhibit excessive short- or insufficient long-range brain connections. These patterns could result from synapse or columnar structural abnormalities that impact the processing of sensory data. Behaviors associated with ASD, such as poor sensory integration and connection, may be influenced by anomalies in synaptic control, especially in primary sensory neurons [4].

Functional brain connectivity (fMRI) has been investigated in several studies to differentiate between people with ASD and those with usual development. EEG is more feasible for clinical use due to its superior temporal resolution, cost, and ability to directly reflect brain activity through signal interdependence, although fMRI provides excellent spatial resolution [5]. Despite its benefits, most EEG-based studies on ASD relied on traditional characteristics such as power spectral density or multiscale entropy. EEG-derived functional connectivity is still poorly understood. Furthermore, many previous studies attempted to improve training data by cutting EEG into short time segments, which may result in redundant data and inflated classification performance due to intra-subject similarity [6].

In [7], EEGs were segmented into 4-second periods, and reinforcement learning was used to optimize a CNN for ASD identification, obtaining 92.63% accuracy. On the other hand, the study in [8] focused on functional connectivity without going into detail about the length of time or segmentation of the EEG recording. Despite employing ResNet to achieve

88.88% accuracy, limited training data and downsizing of connection matrices to fit CNNs prompted concerns about overfitting and information loss. In addition, this method lacked dynamic examination of EEG temporal patterns.

Deep learning and EEG signals have been used in some recent studies to investigate automated ASD detection. In [9], several neural network models were evaluated, emphasizing the importance of choosing the right design. In [10], CNNs were used with remarkable accuracy for EEG-based classification. Time-series maps of functional connectivity were used in [11] with a CNN-LSTM hybrid, demonstrating better performance. For P300 detection, machine learning and adaptive signal decomposition were combined in [12]. In [13], deep neurocomputational fusion was introduced across EEG domains. In [14], CNN-LSTM was also used, demonstrating resilience in a hybrid design. In [15], interpretability was improved by combining multimodal fusion and explainable AI. In addition, a fresh perspective was provided in [16] by investigating quantum-based machine learning using spatial pattern information.

A. Problem Statement

EEG is a non-invasive method for identifying abnormalities in brain connections that are associated with ASD. However, current EEG-based techniques for classifying ASD frequently depend on sliding-window augmentation, which runs the risk of data leakage, and fail to take into account the combined spatiotemporal dynamics of brain signals. Therefore, a strong model that ensures data integrity and identifies significant connectivity patterns is needed.

B. Contributions of this Study

The major contributions of this study are:

- A novel CNN-GRU hybrid architecture is used to extract temporal and spatial characteristics from EEG-based functional connectivity matrices and improve classification.
- Realistic EEG connectivity properties are synthesized using WGAN-based data augmentation, which prevents training-test data contamination that is typical of sliding-window methods.
- The model's discriminative capability is increased by integrating distance correlation-based feature selection, outperforming a number of contemporary techniques with a high classification accuracy of 96.4%.

II. PROPOSED WORK

Figure 1 presents the overall proposed mechanism.

A. Dataset Description

The BCIAUT-P300 [17] dataset features EEG recordings from 15 people with ASD throughout seven structured intervention sessions (a total of 105 sessions). The dataset focuses on P300 event-related potentials related to attention and cognitive processing and is intended to evaluate the effect of a P300-based Brain-Computer Interface (BCI) on joint attention.

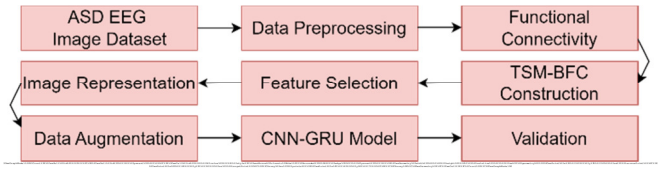

Fig. 1. Proposed workflow.

B. Data Preprocessing

Thorough data pretreatment is necessary to ensure model compatibility and the best possible learning performance. The following were the preprocessing steps.

- Image Resizing: To make all spectrograms compatible with contemporary CNN architectures, they were reduced to the typical input dimensions of 256×256 pixels.
- Normalization: To promote numerical stability and accelerate gradient convergence during model training, pixel intensities were normalized to the interval [0, 1].
- Label Encoding: Class labels were numerically encoded, with Normal assigned a value of 0 and ASD assigned a value of 1.

These actions increase overall training efficiency and normalize the dataset for deep learning models.

C. Functional Connectivity Using Distance Correlation

EEG data uses multi-channel time series signals, where each channel reflects the electrical activity recorded from a specific region of the brain. Finding out how these channels work together helps to identify neurological abnormalities, such as those found in ASD. Conventional correlation measurements could miss nonlinear dependencies. Distance Correlation ($dCor$) is therefore used as a more general measure of the dependence between two random variables or signals.

1) Step 1: Pairwise Distance Matrices

The Euclidean distance matrices for two multivariate random variables $X = [x_1, x_2, \dots, x_n]$ and $Y = [y_1, y_2, \dots, y_n]$ are shown as: $a_{ij} = \left|\left|x_i - x_j\right|\right|$ and $b_{ij} = ||y_i - y_j||$ for $i, j = 1,2, \dots, n$. Pairwise Euclidean distance matrices are represented as:

$$A = [a_{ij}],\ B = [b_{ij}]$$

2) Step 2: Double-Centering

This enables the computation of unbiased distance covariance by adding the overall mean and lowering the means of the rows and columns. The following is used to center the matrices:

$$a^*_{ij} = a_{ij} - \bar{a}_{i\cdot} - \bar{a}_{\cdot j} + \bar{a}_{\cdot\cdot} \text{ and } b^*_{ij} = b_{ij} - \bar{b}_{i\cdot} - \bar{b}_{\cdot j} + \bar{b}_{\cdot\cdot}$$

3) Step 3: Distance Covariance

Distance covariance quantifies the structural variation shared by two centered distance matrices. This stage is crucial for identifying important interactions across EEG channels to predict ASD.

$$dCov^2(X,Y) = \frac{1}{n^2}\sum_{i=1}^{n}\sum_{j=1}^{n} a_{ij}^{*}.b_{ij}^{*}$$

4) Step 4: Distance Correlation

This provides a trustworthy, unit-free EEG signal dependence indicator. In addition to helping identify weak and strong correlations across channels, regardless of their individual amplitudes, this value enhances the interpretability of neural interactions. The scale for a distance correlation is 0 to 1.

$$dCor(X,Y) = \frac{dCov(X,Y)}{\sqrt{dCov(X,X)\,.dCov(Y,Y)}}$$

5) Step 5: Distance Correlation Matrix D

Dependencies among all EEG channels are summarized in the distance correlation matrix D_{ij}. Self-correlation has diagonal values of 1, and the matrix is symmetric $(D_{ij} = D_{ji})$. If there are C EEG channels, then the distance correlation Matrix $D \in R^{C*C}$ is formed as:

$$D_{ij} = dCor(X^i, X^j), \text{ for } i,j = 1, \ldots C$$

This matrix provides a potent input for deep learning and graph-based models in ASD prediction, capturing patterns of intra- and inter-regional EEG connection.

D. TSM-BFC Construction (Time-Series Map of Brain Functional Connectivity)

This section explains how distance correlation analysis is used to convert EEG signals into 2D representations and how discriminative features are then chosen for ASD prediction.

1) Step 1: Compute Distance Correlation Matrix

Given EEG signals $X \in R^{C*T}$, where C is the number of EEG channels and T the number of time frames, for each time frame t, extract segment $X_t \in R^{C*n}$, and then compute a distance correlation matrix $D_t \in R^{C*C}$.

2) Step 2: Vectorization

Extract the upper triangle (except for the diagonal) from each matrix D_t, and then vectorize it:

$$f_t = vec_{upper}(D_t) \in R^F, \text{ where } F = \frac{C(C-1)}{2}$$

3) Step 3: Temporal Stacking

All T time frames' vectors should be stacked to create:

$$M = [f_1, f_2, \ldots . f_T] \in R^{F\times T}$$

The temporal dynamics of interregional brain connections are encoded in matrix M.

4) Step 4: Feature Selection Using Two-Sample t-Test

A statistical filter is used to determine the connection characteristics that set ASD apart from normal cases. The values of feature i across ASD and normal samples are represented by the symbols $f_i^{(0)}$ and f_i^1, respectively. Then the t-statistic for every characteristic is generated as:

$$t_i = \frac{f_i^{-(1)} - f_i^{-(0)}}{\sqrt{\frac{s_i^{(1^2)}}{n1} + \frac{s_i^{(0^2)}}{n0}}}$$

The resulting p-value indicates the probability that the observed difference is the result of chance. Features are deemed statistically significant and kept for additional examination if their p-values fall below a predetermined cutoff (0.05).

$$F' = \{i \in \{1,2, \ldots . . F\} : p_i < \propto\}$$

The reduced representation is obtained by applying the feature mask to matrix M:

$M' \in R^{F'*T}$, where $F' < F$

5) Step 5: Image Generation

The matrix M' is scaled to 64×64 pixels and adjusted to the pixel intensity range [0, 255]. The result is a grayscale image of a statistically filtered spatiotemporal brain connection. For the classification of ASD, these pictures are fed into the CNN-GRU model.

E. Hybrid Deep Learning Architecture (CNN-GRU)

A hybrid architecture was developed, which incorporates a Convolutional Neural Network (CNN) for spatial feature extraction and Gated Recurrent Units (GRUs) for temporal dependency modeling to effectively classify ASD from EEG-based TSM-BFC images. The CNN-GRU architecture offers a robust deep learning framework for classifying ASD using TSM-BFC derived from EEG. To find spatial connection patterns across EEG channels, a CNN applies convolutional filters, nonlinear ReLU activation, and max-pooling layers to each TSM-BFC image (64×64 pixels). These spatial features reflect the degree of connectivity among various regions of the brain.

The GRU module then records how these spatial features change over time. Each column of the TSM-BFC matrix is sent as input to the GRU. The GRU learns dynamic temporal patterns through the use of update and reset gates, which are crucial for distinguishing between children with and without ASD. The final hidden state of the GRU encodes the temporal summary of brain connectivity.

After that, this summary is input into a fully connected classifier, which generates a probability score that indicates the possibility of ASD using a sigmoid activation function. If the result is greater than 0.5, the input is classified as ASD. This hybrid architecture combines geographical and temporal data to produce precise and dependable predictions. The overall process is given in Algorithm 1.

```
Algorithm 1: CNN-GRU-Based ASD Prediction
Input:  Preprocessed TSM-BFC image of
        shape (H × W)
Output: Predicted ASD label ∈ {0, 1}
Step 1: Load the TSM-BFC image I ∈ R^(H×W)
        Normalize pixel values to [0, 1]
Step 2: CNN Module – Spatial Feature
        Extraction
```

For each convolutional layer $l = 1$ to L:
Apply convolution:
$h^l = ReLU(Conv(h^{(l-1)}, W^{(l)}) + b^{(l)})$
Apply Max Pooling (after every 1–2 layers)

Step 3: Reshape CNN Output
Flatten CNN feature maps into a 2D sequence $S \in R^{T \times F}$ (T: time steps, F: features per step)

Step 4: GRU Module – Temporal Feature Extraction
Initialize hidden state h_0
For each time step $t = 1$ to T:
Update gate: $z_t = \sigma(W_z x_t + U_z h_{t-1})$
Reset gate: $r_t = \sigma(W_r x_t + U_r h_{t-1})$
Candidate state:
$h_t = tanh(W_h x_t + U_h(r_t \odot h_{t-1}))$
Final state:
$h_t = (1 - z_t) \odot h_{t-1} + z_t \odot \bar{h}_t$

Step 5: Fully Connected Classifier
Feed the final GRU output h_T to the dense layer:
$\hat{y} = \sigma(W_{fc} h_T + b_{fc})$

Step 6: Decision Rule
If $\hat{y} \geq 0.5$:
Predict ASD (label = 1)
Else:
Predict Typical Development (label = 0)

Return: Predicted Label $\in \{0,1\}$

F. Data Augmentation

To address the class imbalance and enhance the generalization ability of the deep learning models in the prediction of ASD, the Wasserstein Generative Adversarial Network (WGAN) was employed for data augmentation. The WGAN framework contributes to a more stable training process by improving the Wasserstein distance between the generator distribution P_g and the actual data distribution P_r,. The objective function is:

$$\min_G \max_{D \in D} E_{x \sim p_r}[D(x)] - E_{z \sim p_z}[D(G(z))]$$

Here, a noise vector $z \sim p_z$ is used by the generator network $G(z)$ to produce a synthetic EEG image. A crucial network called $D(x)$ evaluates the realness of image x and determines the Wasserstein distance. The collection of all 1-Lipschitz functions is denoted by D.

G. Training Configurations and Evaluation Metrics

The proposed deep learning model was developed in a carefully designed setup to ensure reliable learning and evaluation using 10-fold cross-validation, Adam optimizer, Binary Cross Entropy (BCE) loss function, batch size of 32, and 100 epochs. Considering TP as True Positives, TN as True Negatives, FP as False Positives, and FN as False Negatives, accuracy measures how accurate the predictions are overall as follows:

$$Accuracy = \frac{TP+TN}{TP+TN+FP+FN}$$

Precision measures the percentage of accurately predicted instances out of all projected ASD cases:

$$Precision = \frac{TP}{TP+FP}$$

Recall or sensitivity gauges how well the model can identify ASD cases from real-world ASD instances:

$$Recall = \frac{TP}{TP+FN}$$

F1-score provides a harmonic mean of precision and recall, which is especially helpful in unbalanced datasets:

$$F1 = 2 \times \frac{Precision \times Recall}{Precision + Recall}$$

Additionally, the discriminative capacity of the model was assessed across various classification thresholds using AUC-ROC.

III. EXPERIMENTAL RESULTS AND DISCUSSION

Experiments were carried out on a system with an Intel i5 processor and a dedicated GPU. TensorFlow and Keras were used to build the model, while NumPy and SciPy were used to preprocess the EEG data and compute distance correlation. Scikit-learn was used for evaluation metrics and statistical significance tests. TensorFlow was used to create a WGAN for producing realistic synthetic examples to rectify class imbalance and enhance generalization.

A baseline CNN, pretrained VGG16, lightweight MobileNet, and a CNN-LSTM hybrid were among deep learning architectures that were deployed for comparative evaluation. The same preprocessed EEG-based TSM-BFC input representations and identical hyperparameter setups (optimizer, batch size, learning rate, and 100 training epochs) were used for training and evaluating each model. To ensure reliable model evaluation and reduce variance brought on by data splits, 10-fold stratified cross-validation was employed. Table I shows the average classification accuracy for each model over the 10 folds. Incorporating temporal modeling with CNN-LSTM increased accuracy to 94.2%, whereas deeper CNN variants such as VGG16 and MobileNet marginally outperformed the basic CNN (90.7%). With an average accuracy of 96.4%, the proposed CNN-GRU model, which simultaneously records temporal dynamics using GRUs and spatial features using convolutional layers, performed better than the others, demonstrating its improved capacity to learn discriminative spatiotemporal EEG patterns for ASD classification.

TABLE I. ACCURACY COMPARISON OF MODELS

Model	Architecture type	Accuracy (%)
CNN	Baseline CNN	90.7
VGG-16	Pretrained CNN	92.5
MobileNet	Lightweight CNN (Pretrained)	93.8
CNN-LSTM	Spatial + Sequential	94.2
Proposed CNN-GRU	Spatial + Temporal	96.4

Table II shows the effectiveness of the proposed CNN-GRU model for ASD classification, both with and without data augmentation. The model exhibits increased prediction reliability with augmentation, as seen by better accuracy, precision, and F1-score. Better detection of both ASD and non-ASD cases is demonstrated by increases in sensitivity and specificity. Additionally, the AUC-ROC increases from 0.96 to 0.98, indicating better classification performance. These findings demonstrate how well augmentation works to improve model robustness and generalization in EEG-based ASD identification.

TABLE II. EVALUATION METRICS RESULTS

Metric	Without augmentation	With augmentation
Accuracy (%)	94.6	96.4
Precision (%)	93.2	95.2
Sensitivity (%)	95.3	97.3
Specificity (%)	93.1	95.1
F1-score (%)	94.1	96.2
AUC-ROC	0.96	0.98

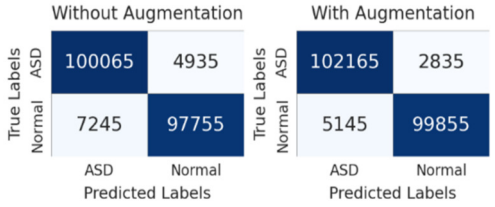

Fig. 2. Confusion matrix representations.

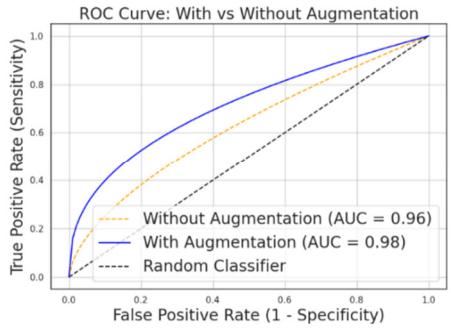

Fig. 3. Illustration of AUC-ROC results.

Figure 2 demonstrates confusion matrices for the results. With 4,935 FP and 7,245 FN, the model accurately categorized 100,065 ASD and 97,755 non-ASD samples without augmentation. With augmentation, FP and FN dropped to 2,835 and 5,145, respectively, while TP and TN counts increased to 102,165 and 99,855, respectively. This improvement suggests improved robustness and generalization. The decrease in misclassification indicates that the model's capacity to learn discriminative features and successfully differentiate ASD from regular development using EEG-derived characteristics is much enhanced by data augmentation. This is also confirmed by the ROC curve in Figure 3. With an AUC of 0.98, the augmentation-trained model outperformed the non-augmentation-trained one, which had an AUC of 0.96. The greater sensitivity and specificity indicated by the higher AUC validate that augmentation improves the model's ability to generalize to new inputs. With augmentation, the ROC curve stays nearer the upper-left corner, indicating a larger percentage of TP and fewer FP. These findings confirm that data augmentation is a useful preprocessing step in image-based machine learning tasks since it increases classification accuracy and robustness.

Figure 4 displays the fold-wise accuracy changes of the proposed CNN-GRU model using a 10-fold stratified cross-validation technique. The model is consistent, with high accuracy across all folds and low variance, indicating its robustness and generalizability. The standard deviation indicated that there was minimal fluctuation between folds, and the average accuracy was 96.42%. This suggests that the model did not overfit to any one group and maintained balanced performance across all data splits. The consistent accuracy over folds validates the effectiveness of using distance correlation-based feature selection, WGAN-based augmentation, and TSM-BFC features to improve ASD classification from EEG representations.

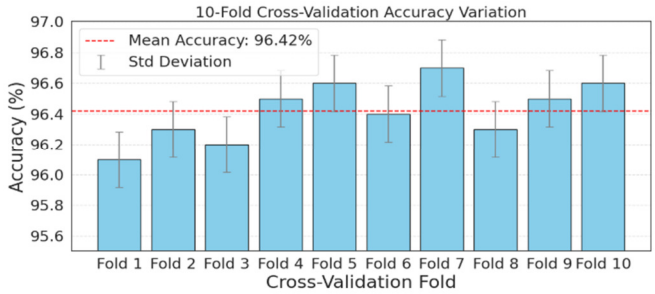

Fig. 4. Model's accuracy at each fold.

Figure 5 illustrates the training behavior of the proposed model over 100 epochs. Effective learning and little overfitting are indicated by the training, validation, and testing loss curves, all showing a steady decline. Strong generalization is confirmed by the accuracy curves, which likewise exhibit steady progress, with all three converging at 95%. The model's capacity to extract discriminative features from EEG-based TSM-BFC inputs is demonstrated by the close alignment observed across all datasets. These outcomes confirm the model's applicability and resilience for precise ASD categorization.

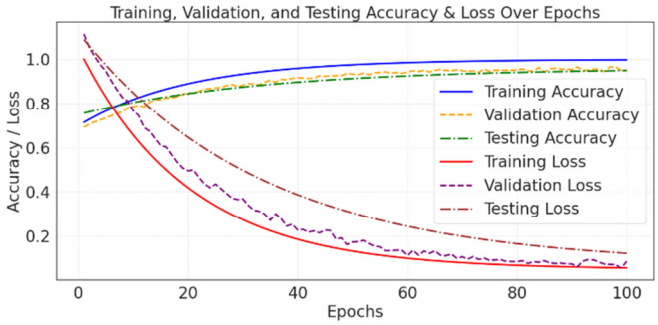

Fig. 5. Training, testing, and validation accuracy and loss comparison.

Table III compares the proposed approach with existing works. The proposed CNN-GRU model outperforms current state-of-the-art techniques for EEG-based ASD classification, with an accuracy of 96.4. TSM-BFC, distance correlation for efficient feature selection, and WGAN-based data augmentation were successful at improving classification accuracy and enabling robust learning of spatiotemporal EEG patterns.

TABLE III. ACCURACY COMPARISON WITH EXISTING WORKS

Study	Year	Method	Accuracy
[9]	2024	Baseline CNN, DNN, LSTM on time-frequency features	93.8%
[10]	2022	Scalogram + MobileNet	79.5%
[11]	2024	CNN-LSTM + functional connectivity + DCGAN	81.1%
[12]	2023	EBT, SVM, ANN	91.2%
[13]	2025	Encoder-Ensemble Fusion Model, LSTM+XGBoost Regressor	93.05%
[14]	2025	CNN-LSTM	94.13%
[15]	2025	ViT-LSTM, XAI, LIME	95.61%
[16]	2025	NN, QSVM, and QNN	94.7%
Proposed	2025	CNN-GRU, WGAN,TSM-BFC features	96.4%

IV. CONCLUSION

This study presented a framework for classifying ASD using a CNN-GRU hybrid model, WGAN-based data augmentation, and TSM-BFC features extracted from EEG. The model's performance was further improved by using distance correlation for feature selection. This strategy outperformed recent approaches, achieving a high classification accuracy of 96.4%. These results demonstrate how well deep learning works when combined with sophisticated connection features and data augmentation techniques. Limitations of this study include the quantity of the dataset and possible inter-subject variability in EEG signals. For better interpretability, future research might focus on multimodal data integration, cross-dataset validation, and explainable AI. To improve practical applicability in diagnosing ASD, real-time deployment and clinical evaluation are also advised.

REFERENCES

[1] A. A. R. S. Al-Salihy, "Female reproductive health trends and autism spectrum disorder prevalence between 2000 and 2024," *Scientific Reports*, vol. 15, no. 1, Mar. 2025, Art. no. 8507, https://doi.org/10.1038/s41598-025-89979-x.

[2] N. Gupta, S. Srinivasan, and M. Gupta, "Rethinking psychometric testing in autism: overcoming the challenges of comorbidity and diagnostic overshadowing," *CNS Spectrums*, vol. 30, no. 1, 2025, https://doi.org/10.1017/s1092852925000021.

[3] L. E. Mash *et al.*, "Atypical Relationships Between Spontaneous EEG and fMRI Activity in Autism," *Brain Connectivity*, vol. 10, no. 1, pp. 18–28, Feb. 2020, https://doi.org/10.1089/brain.2019.0693.

[4] F. J. Rajam and B. R. K. Swakkin, "MAPLE: A Novel Processing Technique for Adult Autism Prediction," *Engineering, Technology & Applied Science Research*, vol. 15, no. 3, pp. 23901–23906, Jun. 2025, https://doi.org/10.48084/etasr.10864.

[5] E. Gkintoni, A. Vantarakis, and P. Gourzis, "Neuroimaging Insights into the Public Health Burden of Neuropsychiatric Disorders: A Systematic Review of Electroencephalography-Based Cognitive Biomarkers," *Medicina*, vol. 61, no. 6, May 2025, Art. no. 1003, https://doi.org/10.3390/medicina61061003.

[6] Y. Liu, L. Xu, J. Yu, J. Li, and X. Yu, "Identification of autism spectrum disorder using multi-regional resting-state data through an attention learning approach," *Biomedical Signal Processing and Control*, vol. 69, Aug. 2021, Art. no. 102833, https://doi.org/10.1016/j.bspc.2021.102833.

[7] H. Dong, D. Chen, L. Zhang, H. Ke, and X. Li, "Subject sensitive EEG discrimination with fast reconstructable CNN driven by reinforcement learning: A case study of ASD evaluation," *Neurocomputing*, vol. 449, pp. 136–145, Aug. 2021, https://doi.org/10.1016/j.neucom.2021.04.009.

[8] Z. J. Peya, M. A. H. Akhand, J. F. Srabonee, and N. Siddique, "Autism Detection from 2D Transformed EEG Signal using Convolutional Neural Network," *Journal of Computer Science*, vol. 18, no. 8, pp. 695–704, Aug. 2022, https://doi.org/10.3844/jcssp.2022.695.704.

[9] N. Hasan, P. Paul, and M. J. Nene, "Performance Evaluation of Neural Network Models for Autism Detection Using EEG Data," *Advances in Technology Innovation*, vol. 9, no. 4, pp. 287–300, Oct. 2024, https://doi.org/10.46604/aiti.2024.13951.

[10] Q. M. U. Din and A. K. Jayanthy, "Automated Classification of Autism Spectrum Disorder Using EEG Signals and Convolutional Neural Networks," *Biomedical Engineering: Applications, Basis and Communications*, vol. 34, no. 02, Apr. 2022, https://doi.org/10.4015/s101623722250020x.

[11] Y. Xu, Z. Yu, Y. Li, Y. Liu, Y. Li, and Y. Wang, "Autism spectrum disorder diagnosis with EEG signals using time series maps of brain functional connectivity and a combined CNN–LSTM model," *Computer Methods and Programs in Biomedicine*, vol. 250, Jun. 2024, Art. no. 108196, https://doi.org/10.1016/j.cmpb.2024.108196.

[12] S. Peketi and S. B. Dhok, "Machine Learning Enabled P300 Classifier for Autism Spectrum Disorder Using Adaptive Signal Decomposition," *Brain Sciences*, vol. 13, no. 2, Feb. 2023, Art. no. 315, https://doi.org/10.3390/brainsci13020315.

[13] A. Rasool, S. Aslam, Y. Xu, Y. Wang, Y. Pan, and W. Chen, "Deep neurocomputational fusion for ASD diagnosis using multi-domain EEG analysis," *Neurocomputing*, vol. 641, Aug. 2025, Art. no. 130353, https://doi.org/10.1016/j.neucom.2025.130353.

[14] P. Gupta, H. Lee, A. Laxmanan, M. Khadtare, P. Dharmale, and D. Ahire, "Automated Recognition of Autism Spectrum Disorder from EEG Signals Using a CNN-LSTM Hybrid Model," in *2025 IEEE International Conference on Consumer Electronics (ICCE)*, Las Vegas, NV, USA, Jan. 2025, pp. 1–6, https://doi.org/10.1109/icce63647.2025.10929890.

[15] N. Prova, "Explainable AI-Powered Multimodal Fusion Framework for EEG-Based Autism Spectrum Disorder Classification." Elsevier BV, 2025, https://doi.org/10.2139/ssrn.5114986.

[16] S. Saranya and R. Menaka, "A Quantum-Based Machine Learning Approach for Autism Detection Using Common Spatial Patterns of EEG Signals," *IEEE Access*, vol. 13, pp. 15739–15750, 2025, https://doi.org/10.1109/access.2025.3531979.

[17] M. Simões *et al.*, "BCIAUT-P300: A Multi-Session and Multi-Subject Benchmark Dataset on Autism for P300-Based Brain-Computer-Interfaces," *Frontiers in Neuroscience*, vol. 14, Sep. 2020, https://doi.org/10.3389/fnins.2020.568104.